

DFT study on the structures and properties of 3-nitro-1,2,4-triazol-5-one crystals at high pressure

Lina Xu^{a,b}, Guoyong Fang^{a,b,*}, Xinhua Li^a, Jixin Yuan^a, Xingen Hu^a,
Weihua Zhu^b, Heming Xiao^b, Guangfu Ji^{b,c}

^a School of Chemistry and Materials Engineering, Wenzhou University, Wenzhou 325035, PR China

^b Department of Chemistry, Nanjing University of Science and Technology, Nanjing 210094, PR China

^c Lab for Shockwave and Detonation Physics, Institute of Fluid Physics, China Academy of Engineering Physics, Mianyang 621900, PR China

Received 28 November 2006; received in revised form 17 January 2007; accepted 18 January 2007

Available online 21 January 2007

Abstract

The geometries, lattice parameters, electronic structures, XRD spectra and optical properties of the 3-nitro-1,2,4-triazol-5-one (NTO) crystals at high pressure (2, 4, 6, 8 and 10 GPa) have been studied using density functional theory within the generalized gradient approximation implemented using ultrasoft pseudo-potentials. The computational results show that with increasing pressure, the NTO lattice parameters and hydrogen bonds lengths rapidly decrease and the geometries change very little. The total energy increases by approximately 27.543 eV from 0 to 10 GPa. NTO becomes increasingly conductive or metallic with increasing pressure, while the XRD peaks are shifted to greater angles and the absorption coefficient $\alpha(\omega)$ increases.

© 2007 Elsevier Inc. All rights reserved.

Keywords: 3-Nitro-1,2,4-triazol-5-one (NTO); Density functional theory; XRD spectra; Optical properties

1. Introduction

3-Nitro-1,2,4-triazol-5-one (NTO) is a well-known insensitive high explosive (IHE). Since this compound was first prepared, it has been investigated in a number of experimental and theoretical studies [1–27]. It was characterized as a potential high energy density material (HEDM) that is powerful yet resistant to accidental and sympathetic initiation. Its crystalline structure has been theoretically and experimentally investigated. Sorescu and Thompson developed an intermolecular potential to describe the structure of NTO crystal using rigid molecules [15]. Xiao used the periodic DFT-B3LYP technique to investigate the intermolecular interaction in the bulk state of NTO [16]. However, to date there has been no report on a systemic study of NTO crystalline structures under high isostatic pressure. Crystalline structures determine

crystalline properties. There is great interest in NTO crystalline structures under high detonation pressures or other extreme conditions, but it is very difficult or impossible to study these experimentally. In this study we used ab initio periodic calculation methods based on density functional theory to study the equilibrium geometries, lattice parameters, electronic structures, XRD spectra and optical properties of NTO crystal at high isostatic pressure. These information will be helpful for the study and molecular design of energetic compounds.

2. Computational methods

The calculations in this study were performed within the framework of DFT [28] using Vanderbilt-type ultrasoft pseudo-potentials [29] and a plane-wave expansion of the wave functions. The self-consistent ground state of the system was determined using a band-by-band conjugate gradient technique to minimize the total energy of the system with respect to the plane-wave coefficients at different external pressures of 0, 2, 4, 6, 8 and 10 GPa. The electronic wave functions were obtained using a density-mixing scheme [30] and the structures were relaxed using the Broyden–Fletcher–Goldfarb–Shannon

* Corresponding author at: School of Chemistry and Materials Engineering, Wenzhou University, Wenzhou 325035, PR China. Tel.: +86 577 88373111; fax: +86 577 88373113.

E-mail address: ahfanggy@sohu.com (G. Fang).

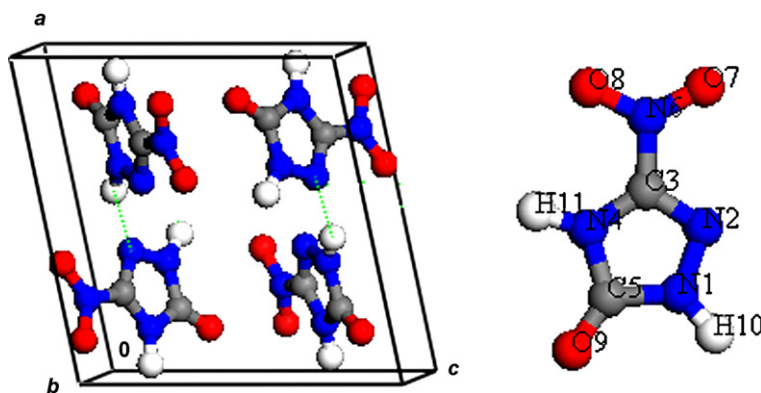


Fig. 1. Packing and atomic numbering of β -NTO in the unit cell. Carbon, nitrogen, oxygen, and hydrogen atoms are represented in gray, blue, red, and white, respectively.

(BFGS) method [31]. The generalized gradient approximation (GGA) with PW91 was employed. We adopted the experimental structure (Fig. 1) from Ref. [5] as the initial structure. All calculations were carried out by using CASTEP code [32]. The cutoff energy for plane waves was set to 300.0 eV. Brillouin zone sampling was performed using the Monkhost–Pack scheme with a k -point grid of $2 \times 4 \times 2$. The values of the kinetic energy cutoff and the k -point grid were determined to ensure the convergence of total energies to within 0.01%. In the geometry relaxation, the total energy of the system converged to less than 1.0×10^{-6} eV, the residual force to less than 0.02 eV/Å, the displacement of atoms to less than 0.001 Å, and the residual bulk stress to less than 0.1 GPa.

3. Results and discussion

3.1. Crystal structure

We concentrated on pressures between 0 and 10 GPa and assumed that there is no phase transition in this region. Full

relaxation of the structure was performed to allow the NTO molecular configurations, cell shape and volume to change. The results for all the geometric parameters, including the lattice vectors, are shown in Table 1.

Table 1 shows that although a , b and c decrease with increasing external pressure, c decreases much more rapidly than a and b and the c/a ratio decreases from 0.990 at 0 GPa to 0.977 at 4 GPa and to 0.969 at 10 GPa, which indicates anisotropic changes in the crystal under high pressures. Another decrease in the NTO crystal size is also revealed by the magnitude of the shortening of hydrogen bonds. Table 1 shows that the O–H hydrogen bond length changes from 1.702 to 1.638 to 1.565 Å as the pressure changes from 0 to 4 to 10 GPa, whereas the N–H hydrogen bond distance changes from 2.090 to 2.004 to 1.879, respectively.

Compared with the changes in lattice parameters and hydrogen bond lengths, the bond lengths within an NTO molecule vary much less (more than 100-fold less) with changes in the external pressure. Some bond lengths, such as C–O and N–H, increase, whereas others, such as C–N, N–N and

Table 1
Cell and geometric parameters for NTO crystals at different external pressures

Parameter	0 (GPa)	2 (GPa)	4 (GPa)	6 (GPa)	8 (GPa)	10 (GPa)	Exp. [5]
a (Å)	9.435	9.312	9.255	9.192	9.134	9.089	9.325
b (Å)	5.591	5.484	5.439	5.398	5.353	5.307	5.450
c (Å)	9.336	9.119	9.040	8.970	8.891	8.806	9.040
b/a	0.593	0.589	0.588	0.587	0.586	0.584	0.584
c/a	0.990	0.979	0.977	0.976	0.973	0.969	0.969
β (°)	101.4	101.4	101.5	101.6	101.6	101.6	101.5
N1–N2 (Å)	1.353	1.353	1.352	1.352	1.351	1.351	1.366
N1–C5 (Å)	1.381	1.379	1.378	1.375	1.372	1.372	1.374
N1–H10 (Å)	1.029	1.033	1.035	1.036	1.039	1.039	1.009
N2–C3 (Å)	1.306	1.306	1.306	1.306	1.305	1.305	1.299
C3–N4 (Å)	1.350	1.348	1.347	1.345	1.341	1.341	1.356
C3–N6 (Å)	1.416	1.414	1.413	1.411	1.408	1.408	1.443
N4–C5 (Å)	1.376	1.373	1.371	1.369	1.366	1.366	1.375
N4–H11 (Å)	1.051	1.052	1.054	1.057	1.061	1.061	1.009
C5–O9 (Å)	1.230	1.232	1.232	1.232	1.234	1.234	1.234
N6–O7 (Å)	1.252	1.251	1.251	1.251	1.250	1.250	1.227
N6–O8 (Å)	1.248	1.248	1.248	1.247	1.247	1.247	1.225
N···H (Å)	2.090	2.045	2.004	1.964	1.918	1.879	2.054
O···H (Å)	1.702	1.667	1.638	1.607	1.582	1.565	1.723

Table 2

Total energy and density of crystalline NTO at different external pressures

	0 (GPa)	2 (GPa)	4 (GPa)	6 (GPa)	8 (GPa)	10 (GPa)
Energy (eV)	−10982.058	−10976.291	−10970.652	−10965.147	−10959.772	−10954.515
Density (g/cm ³)	1.850	1.893	1.937	1.981	2.028	2.076

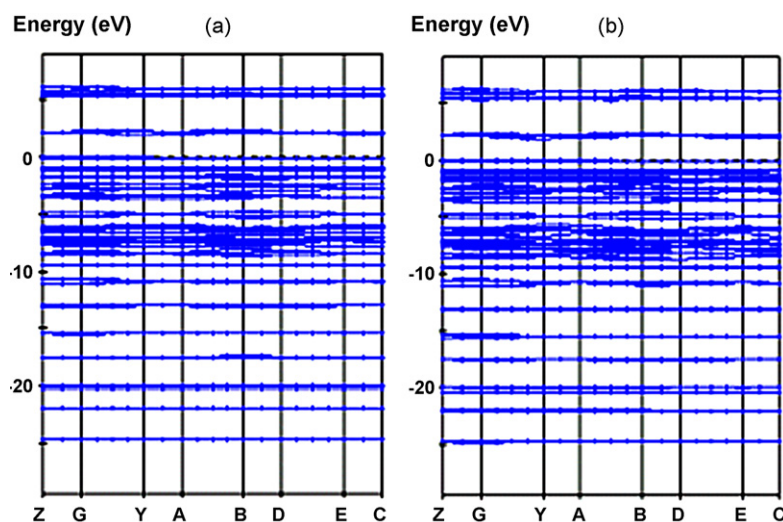


Fig. 2. Energy band structure of NTO at (a) 0 GPa and (b) 10 GPa.

N–O, decrease when the external pressure increases. This trend is in agreement with the well-known donor–acceptor theory [33], which predicts a shorter C–N and longer C–O bond length for stronger hydrogen bonds caused by the charge flow from the C–O bond to oxygen and from nitrogen to the C–N bond. This charge flow is caused by shortening of the hydrogen bond.

3.2. Total energy and density

The total energy and density of NTO crystals at different external pressures from 0 to 10 GPa are listed in Table 2. The total crystal energy and density increase with the external pressure. Total energy is lowest without external pressure (−10980.858 eV), and increases by approximately 27.543 eV from 0 to 10 GPa. The NTO crystal density under typical conditions is 1.850 g/cm³. From the viewpoint of total energy, we can compress an NTO crystal and obtain a crystal density >2.076 g/cm³ at approximately 10 GPa.

3.3. Electronic structures

The energy band structures of NTO crystals at 0 and 10 GPa are shown in Fig. 2 and the energy gaps (E_g) of NTO crystals at

different external pressures are listed in Table 3. The origin of the energy is taken to be the Fermi level. Both the upper valence bands and the lower conduction bands are generally quite flat. The energy gap (E_g) without external pressure is 2.049 eV, indicating that the compound is between an insulator and a semiconductor, which is in agreement with the experiment result [20]. The energy gap decreases with increasing pressure to values that are typical for semiconductors. This demonstrates that NTO becomes increasingly conductive or metallic with increasing pressure, indicating that NTO may change from a semiconductor to a conductor.

3.4. XRD spectrum

Table 4 shows the calculated XRD spectra of NTO crystals under different pressures. These calculated spectra reflect the characteristics of the NTO crystal. The spectra at different pressures are similar, although all 2θ peaks move to greater angles with increasing pressure.

3.5. Optical properties

In this section, we investigate the optical properties of NTO. The interaction of a photon with electrons in the system can result in transitions between occupied and unoccupied states. The spectra resulting from these excitations can be described as a joint density of states between the valence and conduction bands. The imaginary part $\epsilon_2(\omega)$ of the dielectric function can be obtained from the momentum

Table 3

Energy gap of NTO at different isostatic pressures

Pressure (GPa)	0	2	4	6	8	10
Energy gap (eV)	2.049	1.983	1.963	1.947	1.928	1.902

Table 4

Calculated XRD spectra and the four most intense 2θ peaks for NTO crystals at high isostatic pressure

Pressure (GPa)	XRD spectra	2θ peaks ($^{\circ}$)
10		19.95, 26.95, 29.95, 35.50
8		19.85, 26.70, 29.65, 35.15
6		19.70, 29.40, 26.45, 34.80
4		19.5, 26.25, 29.20, 34.55
2		19.45, 26.05, 29.00, 34.20
0		19.30, 25.85, 28.70, 33.95

matrix elements between the occupied and unoccupied wave functions within the selection rules. The real part $\varepsilon_1(\omega)$ of the dielectric function can be calculated from the imaginary part using the Kramer–Kronig relationship. The absorption coefficient $\alpha(\omega)$ can be evaluated from $\varepsilon_1(\omega)$ and $\varepsilon_2(\omega)$ [34].

The absorption coefficient $\alpha(\omega)$ of NTO at different external pressures is plotted in Fig. 3. The first absorption peak in the $\alpha(\omega)$ spectra without external pressure is found at 4.23 eV. The absorption coefficient of the band at 4.23 eV is estimated by our calculations to be $0.7 \times 10^7 \text{ m}^{-1}$. The magnitude of the absorption coefficient ($1.1 \times 10^7 \text{ m}^{-1}$) of the middle absorption peak (at 5.89 eV) indicates an allowed optical transition, probably to an exciton level. We also note that NTO has a very strong adsorption at 8.96 eV. The magnitude of the absorption coefficients of these peaks allows an optical transition due to excitons. Since the absorption coefficient in the fundamental region is very high (10^7 m^{-1}), NTO is unstable and decomposes under the action of light and heat. The absorption peaks for NTO without pressure and at high pressure are at the same energy, whereas, the absorption coefficient increases with pressure. This indicates that the crystal structure of NTO is not destroyed under 10 GPa of external pressure, which is

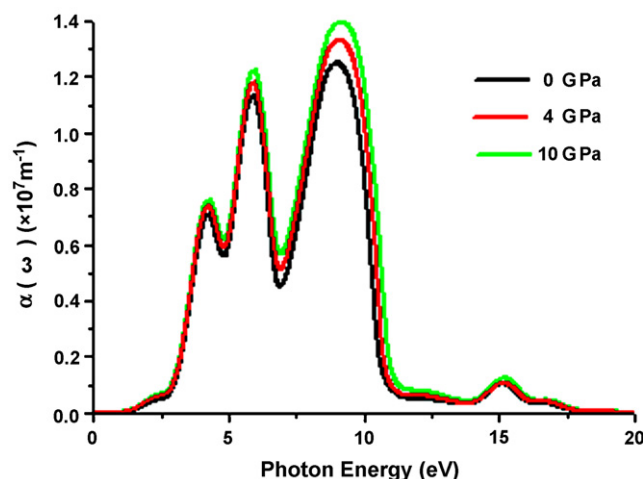


Fig. 3. Optical absorption coefficients of NTO crystal at high isostatic pressure.

consistent with results for the geometry and electronic structure. In conclusion, the absorption spectrum of NTO displays a number of absorption peaks in the fundamental absorption region that are believed to be associated with different exciton states.

4. Conclusions

DFT calculations to investigate the geometries, lattice parameters, electronic structures, XRD spectra and optical properties of NTO lead to the following conclusions:

- (1) The NTO lattice parameters and hydrogen bonds lengths rapidly decrease and the geometries change very little when the pressure increases from 0 to 10 GPa.
- (2) The total crystal energy and density of NTO increase when the external pressure increases. The total energy increases by approximately 27.543 eV from 0 to 10 GPa and NTO can be compressed to a crystal density of $>2.076 \text{ g/cm}^3$ in the vicinity of 10 GPa.
- (3) NTO becomes increasingly conductive or metallic with increasing pressure, indicating that it may change from a semiconductor to a conductor.
- (4) The XRD spectra of NTO crystal under different pressure are similar, although the 2θ peaks are shifted to greater angles with increasing pressure.
- (5) The absorption peaks of NTO at low and high pressure are similar and the absorption coefficient $\alpha(\omega)$ increases with increasing pressure.

Acknowledgement

The authors thank the National Natural Science Foundation of PR China (Grant No. 10576016) for financial support.

References

- [1] T.B. Brill, P.E. Gongwer, G.K. Williams, J. Phys. Chem. 98 (1994) 12242.
- [2] L.N. Xu, H.M. Xiao, G.Y. Fang, X.H. Ju, Chim. Acta Sin. 63 (2005) 1062.

- [3] K.Y. Lee, L.B. Chapman, M.D. Coburn, J. Energetic Mater. 5 (1987) 1987.
- [4] E.F. Rothgery, D.E. Audette, R.C. Wedlich, D.A. Csejka, Thermochim. Acta 185 (1991) 235.
- [5] E.A. Zhurova, A.A. Pinkerton, Acta Crystallogr. B: Struct. Sci. 57 (2001) 359.
- [6] A. Finch, P.J. Gardner, A.J. Head, H.S. Majdi, J. Chem. Thermodyn. 23 (1991) 1169.
- [7] J.A. Menapace, J.E. Martin, D.R. Bruss, R.V. Dascher, J. Phys. Chem. 95 (1991) 5509.
- [8] B.C. Beard, J. Sharma, J. Energetic Mater. 11 (1993) 325.
- [9] S. Gurdip, F.S. Prem, J. Mol. Struct. 649 (2003) 71.
- [10] S. Gurdip, F.S. Prem, Combust. Flame 135 (2003) 145.
- [11] T.B. Brill, T.L. Zhang, B.C. Tappan, Combust. Flame 121 (2000) 662.
- [12] J.P. Ritchie, J. Org. Chem. 54 (1989) 3553.
- [13] H. Östmark, H. Bergman, G. Ågvist, Thermochim. Acta 213 (1993) 165.
- [14] N.J. Harris, K. Lammertsma, J. Am. Chem. Soc. 118 (1996) 8084.
- [15] D.C. Sorescu, D.L. Thompson, J. Phys. Chem. B 101 (1997) 3605.
- [16] H.M. Xiao, X.H. Ju, L.N. Xu, G.Y. Fang, J. Chem. Phys. 121 (2004) 12523.
- [17] C. Meredith, T.P. Russell, R.C. Mowrey, J.R. McDonald, J. Phys. Chem. A 102 (1998) 471.
- [18] Y.M. Wang, C. Chen, S.T. Lin, J. Mol. Struct. (Theochem.) 460 (1999) 79.
- [19] W.L. Yim, Z.F. Liu, J. Am. Chem. Soc. 123 (2001) 2243.
- [20] J.R. Song, Investigation on NTO-metal Coordinates, Chemical Industrial Press, Beijing, 1998.
- [21] J.R. Song, Z.X. Chen, R.Z. Hu, H.M. Xiao, F.P. Li, J. Therm. Anal. Calorim. 58 (1999) 257.
- [22] J.R. Song, Z.X. Chen, H.M. Xiao, R.Z. Hu, F.P. Li, Chin. Sci. Bull. 44 (1999) 214.
- [23] J.R. Song, H.X. Ma, J. Huang, Sci. China B 46 (2003) 302.
- [24] J.R. Song, Z.X. Chen, H.M. Xiao, R.Z. Hu, F.P. Li, Acta Chim. Sin. 56 (1998) 270.
- [25] H.X. Ma, J.R. Song, W. Dong, R.Z. Hu, G.H. Zhai, Acta Chim. Sin. 62 (2004) 1139.
- [26] Y.M. Yang, T.L. Zhang, J.G. Zhang, B. Shao, K.B. Yu, Chin. J. Struct. Chem. 21 (2002) 321.
- [27] D.C. Sorescu, T.R.L. Sutton, D.L. Thompson, D. Beardall, C.A. Wight, J. Mol. Struct. 384 (1996) 87.
- [28] M.C. Payne, M.P. Teter, D.C. Allan, T.A. Arias, J.D. Joannopoulos, Rev. Mod. Phys. 64 (1992) 1045.
- [29] D. Vanderbilt, Phys. Rev. B 41 (1990) 7892.
- [30] G. Kresse, J. Furthmüller, Phys. Rev. B 54 (1996) 11169.
- [31] T.H. Fischer, J. Almlof, J. Phys. Chem. 96 (1992) 9768.
- [32] M.D. Segall, P.L.D. Lindan, M.J. Probert, C.J. Pickard, P.J. Hasnip, S.J. Clark, M.C. Payne, J. Phys.: Cond. Matt. 14 (2002) 2717.
- [33] V. Guttman, The Donor–Acceptor Approach to Molecular Interactions, Plenum Press, New York, 1978.
- [34] S. Saha, T.P. Sinha, Phys. Rev. B 62 (2000) 8828.